International Journal of Nanoelectronics and Materials
IJNeaM
ISSN 1985-5761 | E-ISSN 2232-1535

Fabrication and simulation of silicon nanogaps pH sensor as preliminary study for Retinol Binding Protein 4 (RBP4) detection

M. I. Hashim [b], M. N. M. Nuzaihan [a] *, M. F. M. Fathil [a], M. Shaifullah A.S [a], C. Y. Chean [b], N. H. A. Halim [a], Z. Zailan [b], M. K. Md Arshad [a,b], M. Isa [a], Azhari A. W. [c,d], M. Syamsul [e,f], and Rozaimah A.T. [g]

[a]*Institute of Nano Electronic Engineering, Universiti Malaysia Perlis, 01000 Kangar, Perlis, Malaysia*
[b]*Faculty of Electronic Engineering & Technology, Universiti Malaysia Perlis, 02600 Arau, Perlis, Malaysia*
[c]*Faculty of Civil Engineering and Technology, Universiti Malaysia Perlis, 02600, Jalan Kangar-Arau, Perlis Malaysia*
[d]*Center of Excellence for Water Research and Environmental Sustainability Growth (WAREG), Universiti Malaysia Perlis*
[e]*Institute of Nano Optoelectronics Research and Technology, USM, 11900 Pulau Pinang, Malaysia*
[f]*Faculty of Science and Engineering, Waseda University, Shinjuku, Tokyo 169-8555, Japan*
[g]*Bandar Baharu District Health Office, 09800 Serdang, Kedah*
** Corresponding author. Tel.: +60124296433; e-mail: m.nuzaihan@unimap.edu.my*

Received 22 September 2023, Revised 22 July 2024, Accepted 24 August 2024

ABSTRACT

In this research, a silicon nanogap biosensor has the potential to play a significant role in the field of biosensors for detecting Retinol Binding Protein 4 (RBP4) molecules due to its unique nanostructure morphology, biocompatibility features, and electrical capabilities. Additionally, as preliminary research for RBP4, a silicon nanogap biosensor with unique molecular gate control for pH measurement was developed. Firstly, using conventional lithography followed by the Reactive-ion etching (RIE) technique, a nanofabrication approach was utilized to produce silicon nanogaps from silicon-on-insulator (SOI) wafers. The critical aspects contributing to the process and size reduction procedures were highlighted to achieve nanometer-scale size. The resulting silicon nanogaps, ranging from 100 nm to 200 nm, were fabricated precisely on the device. Secondly, pH level detection was performed using several types of standard aqueous pH buffer solutions (pH 6, pH 7, pH 12) to test the electrical response of the device. The sensitivity of the silicon nanogap pH sensor was 7.66 pS/pH (R^2 = 0.97), indicating that the device has a wide range of pH detecting capacity. This also includes the silicon nanogap biosensor validated by simulation, with the sensitivity obtained being 3.24 μA/e.cm^2 (R^2 = 0.98). The simulation of the sensitivity is based on the interface charge (Qf) that represents the concentration of RBP4. The results reveal that the silicon nanogap biosensor has excellent characteristics for detecting pH levels and RBP4 with outstanding sensitivity performance. In conclusion, this silicon nanogap biosensor can be used as a new electrical RBP4 biosensor for biomedical diagnostic applications in the future.

Keywords: *Silicon nanogaps, Diabetes mellitus, Retinol Binding Protein 4, Electrical detection, Interface charge*

1. INTRODUCTION

In the world, obesity, or type 2 diabetes (T2D) are common illness, and the statistics of patients suffering from this disease are growing. T2D is the most important healthcare problem, meaning it is the worldwide rising incidence of disease [1]. Type 2 diabetes mellitus (DM) is a complex disorder that affects nearly every tissue and organ system going well beyond abnormal glucose metabolism through metabolic complications. While not all identified T2D biomarkers are useful for disease diagnosis and action at earlier stages, they will be reported for T2D. In particular, molecules such as proteins, antibodies, enzymes, DNA/RNA probes, phage-derived biomolecular recognition probes, and an appropriate detection method can be collected by the simple biosensor framework [2]. As a powerful way to boost device efficiency while minimizing device scale, cost, and manufacturing times, nano biosensors are emerging. Through engineering the distance for the technology, the nanostructure device is also able to detect the presence of Retinol Binding Protein 4 (RBP4) as a diabetes mellitus (DM) biomarker. In the investigation of T2D, RBP4 is a useful biomarker since its serum level is higher in insulin-resistant cases. Today, several strategies have been developed around the world to diagnose RBP4 as a biomarker of Diabetes Mellitus (DM), such as an enzyme-linked immunosorbent assay (ELISA) [3], an enzyme-linked antibody-aptamer sandwich assay (ELAAS) [4] and surface plasmon resonance (SPR). However, these techniques, especially in the identification of RBP4, have their own challenges. The feasibility of a label-free, rapid, reversible, and sensitive system to identify serum RBP4 should be considered. The problems in quantification, the false positive arising from the identification of sample contamination, is the challenges of the system for the detection of RBP4 have also been established [2]. In this regard, vital biomedical mechanisms, such as blood glucose (protein) sensors, cardiac pacemakers, and deep-brain stimulators, have resulted in the development of bioelectronics. Now with the shrinking of the electronic transducer range to the nanoscale, the size has been decreased, and making their properties look more biological will result in major susceptibility and biocompatibility enhancements and thereby open up

convenience in basic biology and healthcare. The latest advancement in nanotechnology offers a modern medium for mark-free identification of biomolecules at ultra-low combinations. Nanogap biosensors are developed as an effective approach to improving system achievement while reducing device scale, cost, and fabrication times [5]. Due to the ease of measuring, low-cost facilities required, and compatibility with multiplex formats, silicon nanogap biosensors have demonstrated an outstanding approach to detecting biomolecular interactions such as protein. These advantages also result in label-free aptamer-based protein identification for proof of concept in the fabrication of the nanostructure and its detection.

Recently RBP4 has gained consideration as an excellent marker for DM. RBP4 binds specifically with retinol and transports it in the bloodstream to the liver. Elevated serum levels of RBP4 have been found in insulin-resistant humans with obesity and diabetes causing dysfunctions in the production of glucose transporter 4 and ultimately leading to failure of glucose uptake from blood.

Figure 1 shows the RBP4 structure. It is an indicator of the onset of T2D in the future. At present, RBP4 is thought to be a possible biomarker for early T2D management. T2D, since it causes insulin resistance in the human body, is one of the biggest threats to mankind [4]. Some innovative methods have been reported for the detection of RBP4 in serum samples, like a novel aptamer-based Surface Plasmon Resonance (SPR) biosensor [6], in which a gold chip was functionalized with RBP4- specific and used for SPR-based label-free detection of RBP4. To solve the current problem of RBP4 detection, this research is expected to be the best option, promising the realization of silicon nanogap in the development of next-generation diabetes biosensors.

The name pH is derived from the letters oh p and H, which stand for power and hydrogen, respectively [7]. It can be derived in terms of the equation between the water (H_2O), acid (H^+), and alkali (OH^-). The pH scale is used to describe the acidity or basicity of an aqueous solution at an exact temperature. Because pH indicates the number of accessible hydrogen ions rather than the concentration of hydrogen ions, the word activity is utilised. In order to determine a texture chemical property, pH must be measured. pH affects the solubility of various chemicals and biomolecules in any solution, as well as the momentum or rate of biochemical feedback. Controlling the pH is also critical for optimising the desired feedback and preventing undesirable feedback. There are many detection methods that have been used to detect pH in recent years, for example, optical fibre-based pH sensors and metal oxide sensors [7]. The pH measurement is the most widely used test for biosensor detection.

The nanogap refers to an arrangement of a pair of electrodes split by the gap size of the nanometer. Nanogap is a basic block for the manufacture of nanodevices and circuits capable of tuning the electrical properties of a solution or sample of a biomolecule. The useful, stable and higher-sensing technology of Nanogap is increasingly known. Another potential aim is to analyse a single

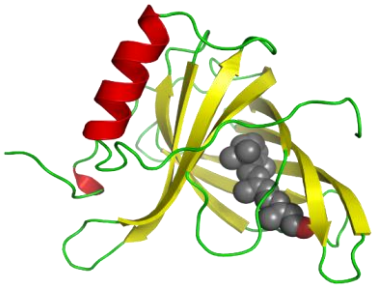

Figure 1. RBP4 structure [5]

molecule's bioactivity and research the reaction. To integrate the biological system with a nanogap, it is necessary to carefully consider the variations between the sensor surface and the electrode [8]. In addition, the dielectric properties between the planar nanogap with and without a sample must be studied. Nanogap devices are compact and provide the possibility for non-volatile memory, small size and operation over a large variety of applications to achieve high switching speed. Two types of nanogap structures, which are vertical and horizontal nanogaps, have been developed worldwide.

A structure with two electrodes vertically positioned in a perpendicular direction is a vertical nanogap. As shown in Figure 2, the vertical nanogap is divided into two classes, which are two terminals and three terminals [9]. The vertical nanogap system is capable of solving the problems of the original feature's high-density arrangement and uniformity, but it also has its difficulties, such as multilayer construction and miniaturization of nanogap components. A system that has both electrodes facing each other horizontally in the configuration of the device is a horizontal nanogap, as shown in Figure 3. In addition, the horizontal nanogap device is useful for fundamental analysis but is not ideal for the integration system because due to the roughness of the electrode edge, the gap distance is uneven.

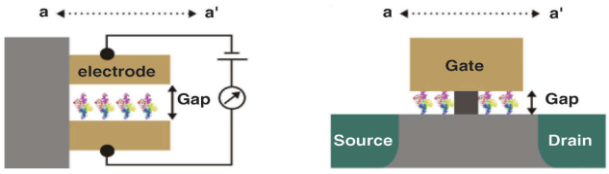

Figure 2. Schematic of field-effect transistor with vertical nanogap [9]

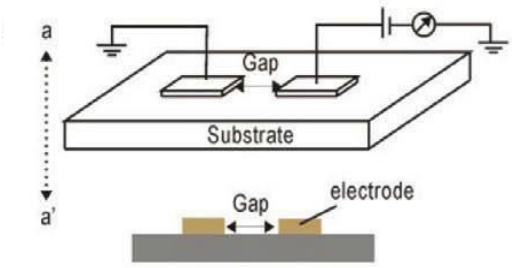

Figure 3. Schematic of field-effect transistor with horizontal nanogap [9]

A highly sensitive silicon nanogap biosensor (silicon as sensing electrode) has been established for diabetes-related RBP4 identification. Silicon has a wide variety of voltage and current handling capacities. For example, it can be used for many purposes for semiconductor devices and integrated circuits, meaning the integration of complicated microelectronic circuits, but quickly assisted. Other than that, the explanation for selecting silicon is conveniently produced and very well interconnected with standard semiconductor processing phases. Moreover, to prevent the growth of outbreaks, ways for identifying RBP4 at a very early stage are crucially required. Proposing a silicon nanogap biosensor is one of the better ways to curb the problem.

As shown in Figure 4, it is a device that defines the point between the two terminals by measuring the electrical parameters for current, resistance, conductance, capacitance, permittivity, and impedance with two electrodes with a nanometer difference scale in the centre [10]. A silicon nanogap biosensor for RBP4 detection has not yet been tested to the best of our understanding. Due to the intrinsic high sensitivity and ability of electrical biosensor mechanisms based on nanogap to minimise and investigate vast numbers of victims' adversity from diabetes, we show the fabrication of silicon nanogap and the electrical detection of RBP4 using this fabrication of silicon nanogap. The change of electricity is dependent on changes in the device's current, resistance and conductance. The performance and sensitivity are measured on the basis of the electrical biosensor as a function of the extension and accuracy of the predictor. The sensitivity word itself reflects the minimal volume of research that can be observed or found by the biosensor. It is also an important output parameter when fabricating the biosensor. As always, the key performance indicator for evaluating any project is its superiority compared to others, particularly in terms of sensitivity. The comparison between the sensitivity and detection system obtained by the current biosensor is reported in the literature as shown in Table 1. The analytical parameters such as transduction type, target, sensitivity concentration and assay principle are presented. Therefore, the efficacy of developing a silicon nanogap biosensor for detecting RBP4 tracking in actual patient samples was demonstrated by the function as shown in the table to give better results in sensitivity. Torabi and Ghourchian [11] reported that the aptasensor detected RBP4 with a sensitivity range of 0.001 to 2 ng/mL. The suggested approach has been used to accurately quantify RBP4 levels in patient samples. It is feasible to create a more usable surface for immobilising luminol and improve

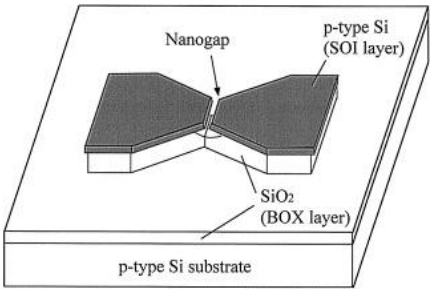

Figure 4. 3D structure of silicon nanogap [10]

chemiluminescence detection by employing intercross-linked gold nanoparticles. Lee et al. [6] reported that this method's sensitivity for all 3 proteins was increased by at least 20-fold to up to 68-fold over the surface plasmon resonance (SPR) approach, which solely utilises aptamers as traps examined. Furthermore, each adipokine spiked in diluted people's serum was detected with identical sensitivity using this test technique. Yang et al. [12] reported that the creation of a new qMSIA for measuring overall and proteolyzed variants of RBP4 is described. In similar serum aliquots from insulin-sensitive individuals with impaired glucose tolerance or T2D, qMSIA and qWestern of RBP4 were conducted. Based on the literature mentioned above, this research demonstrated the performance of silicon nanogap biosensors for the electrical detection of RPB4 as a DM biomarker. This project is expected to be a better solution to resolve the problem of sensitivity and other issues of DM detection. Perhaps the next generation of silicon nanogap biosensors can be developed to achieve high sensitivity in detecting DM.

2. METHODS

The overall fabrication and simulation processes of silicon nanogaps are explained in this section.

2.1. Fabrication of the Silicon Nanogaps pH Sensor

The silicon prime wafer as substrate was cleaned before undergoing the conventional lithography process. RCA-1 (mixing DI water: 5, ammonium hydroxide (27%): 1 and hydrogen peroxide (30%): 1) solution was used to remove surface contaminants from the wafer while RCA-2 (mixing DI water: 6, hydrochloric acid (30%): 1 and hydrogen peroxide (30%): 1) solution used to remove metallic contaminants from the wafer. Then followed by soaking in dilute hydrogen fluoride (HF) to remove the native oxide. The wafer was cut into 2 cm x 2 cm then followed by oxidation process for 1 hour. Next, a 200 nm polysilicon

Table 1. Comparison between the sensitivity and detection system obtained by the current RBP4 biosensor

Detection Method	Target	Sensitivity	Assay Principle	References
Spectroscopy	ssDNA Aptamer	0.001-2 ng/mL	CV	[11]
Spectroscopy	ssDNA Aptamer	78 ng/mL to 5 µg/mL	CV	[6]
Electrochemical	Antibody	0.01-1000 pg/mL	I-V	[12]

layer was deposited on the top of the oxide layer by using low-pressure chemical vapour deposition (LPCVD). In the conventional lithography stage, the sample began with positive photoresist spin-coating via spin-coater for 30 seconds at 5000 rpm and then the resist was soft-baked on the hot plate at 90°C for 90 seconds to enhance the adhesion of the photoresist to the wafer surface. Then the sample was exposed to ultraviolet (UV) light for 110 seconds to transfer the pattern from the chrome mask to the photoresist surface. The exposed area of the photoresist is soluble due to the positive photoresist used and the soluble areas were developed using approximately 35 seconds of developer (RD6) and rinsed with DI water. After the development process, a high-power microscope (HPM) was used to inspect the pattern of nanogaps and then the hard bake process was taken at 90°C for 1 minute to improve the adhesion of the resist to the sample surface. Next, RIE was used to etch the pattern of silicon nanogaps for 7 seconds at 3.5 mTorr of chamber pressure after 10 minutes of cooling down.

Then, the remaining photoresist was completely stripped using acetone and rinsed with DI water. Next, the structure of silicon nanogaps was inspected by HPM. The samples, then undergo a metallization process to develop a contact pad by Aluminium to form the drain terminal and source terminal. The formation of the contact pad is taken by the lift-off method with physical vapour deposition (PVD). Finally, the electrical characteristics of silicon nanogaps were analyzed by observing the current-voltage (I-V) curve of pH sensing and determining the performance of the nanogaps. Figure 5 shows the overall flowchart of the silicon nanogaps fabrication while Figure 6 shows the process flow (cross-section).

2.2. Simulation of the Silicon Nanogaps Biosensor

In this project, the Silvaco ATLAS device simulator is used to simulate the silicon nanogaps biosensor as shown in Figure 7.

The structure was designed by using the parameter in Table 2. It was done by specifying the mesh via coding in the Deckbuild section of the Silvaco Atlas. The suggested mesh must match and cover the whole 3-dimensional silicon nanogaps-based biosensor construction. After that, the mesh location was split into specified numbered regions, and material declarations for each region were completed. Next, the electrodes were chosen and placed on the source and drain regions. The source and drain regions were doped with a p-type concentration of 8×10^{19} cm^{-3} to enable electrical conduction and facilitate the device's function as a sensor. The simulation was then conducted according to different concentrations of interface charge density, Qf as represented by the biomolecular interaction charge during the actual experiment. The simulated electrical characteristics are analysed to evaluate the current and sensitivity of the simulated silicon nanogap biosensor.

Table 2. 3D Design parameter of silicon nanogap

Aspect	Dimension W × L × T (µm)
Aluminium	1 × 0.475 × 0.02
Nanogap	0.3 × 0.05 × 0.05
Oxide	1 × 2 × 3
Substrate (Si)	1 × 2 × 3

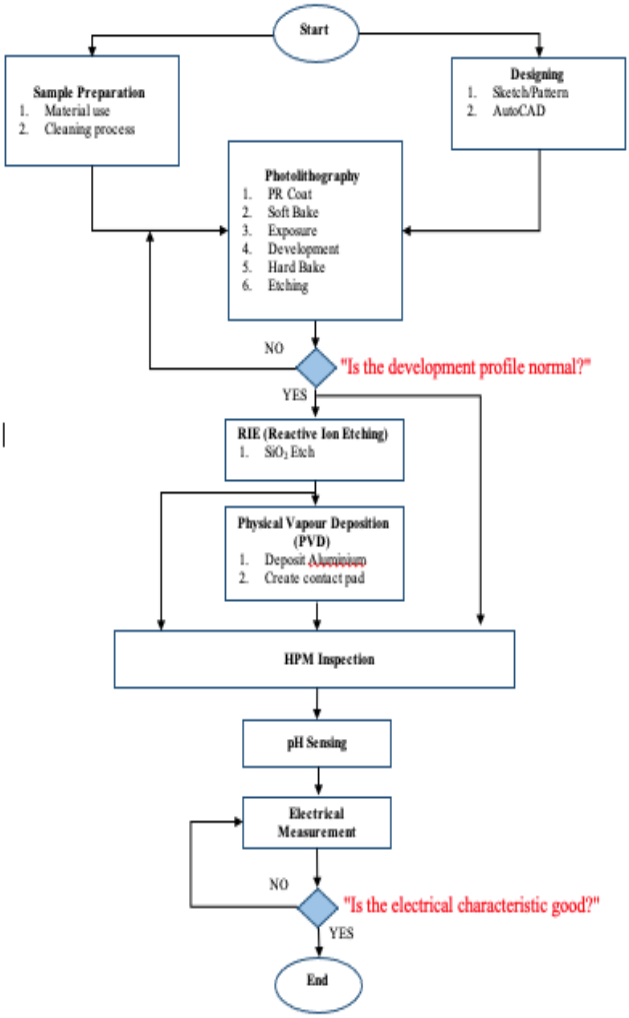

Figure 5. The overall flowchart for the fabrication of silicon nanogaps pH sensor

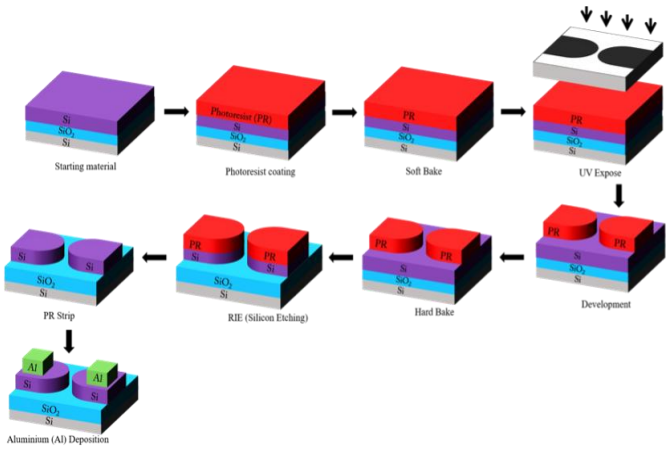

Figure 6. The fabrication process flow (cross-section) of silicon nanogaps pH sensor

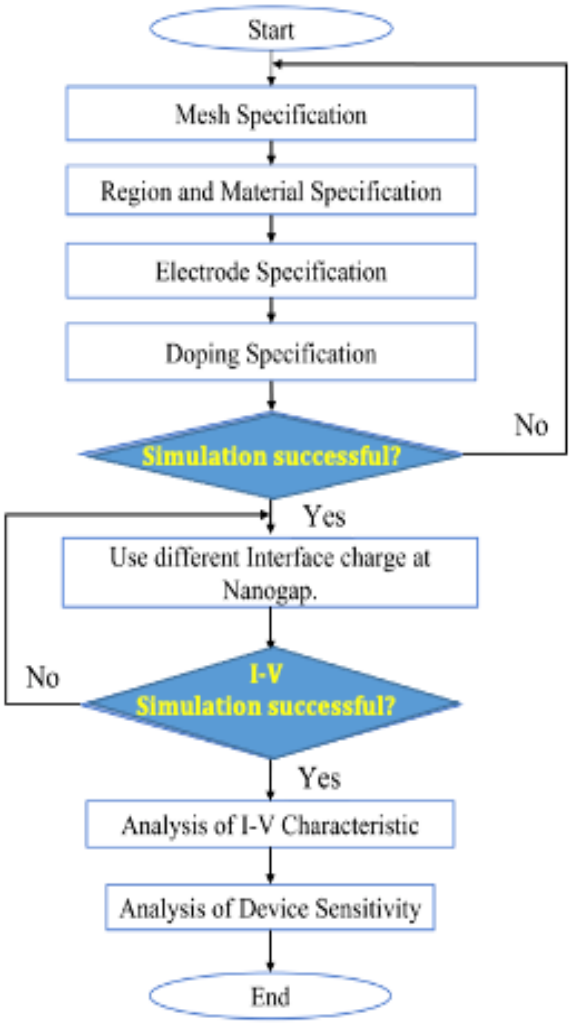

Figure 7. The overall flowchart of the silicon nanogaps simulation using Silvaco ATLAS

2.3. Sensitivity Analysis

The curve calibration (slope) of linear regression from the current against interface charge, Qf graph was used to assess the sensitivity of the structure silicon nanogaps biosensor at varied interface charges. The graph was also drawn within Origin, which included data analysis and interactive scientific graphing. The following equation was used to represent the RBP4 sensor's sensitivity for this project (simulation):

$$\text{Sensitivity} = \frac{\Delta \text{ Current } (A)}{\Delta \text{ Negatively Interface charge, Qf } (\text{e.cm}^2)} \quad (1)$$

The sensitivity obtained was determined by the performance of the sensor in the detection of RBP4. If the sensitivity of the sensor is high, the selectivity also be high. That means the sensor provides the operation result in real time.

3. RESULTS AND DISCUSSION

3.1. Morphological Characterization of the Silicon Nanogaps

The morphology of the silicon nanogaps was investigated using HPM, as it provides direct visualization of the shape, size and uniformity of nanogaps. As shown in Figure 8(b), a normal-develop profile of photoresist nanogaps was developed, while Figure 8 (b) shows the cross-section of silicon nanogaps. The normally developed resist patterns are required to achieve better resolution for the next step which is the RIE process.

Figure 9 (a) and (b) show an anisotropic etching results of nanogaps and its cross-section at A-A'. Based on the obtained results (after the RIE process), the gap of the structure was approximately 200 nm. The images show that a gap is formed with a normal development profile with desirable resolution, good pattern placement and good uniformity [10].

For further information on the morphology of the silicon nanogaps, we previously reported the top-down nanofabrication method of the silicon nanogaps elsewhere [10]. Here, we summarize the main steps of the fabrication process (conventional lithography process, RIE and metal electrode pad formation).

3.2. Electrical Characterization and Sensitivity of the Silicon Nanogaps pH sensor

The pH was electrically characterized to determine the sensor's functionality by using a direct current (DC) voltage that was swept from 0 V to 2 V. Figure 10 shows the I-V characteristic of the silicon nanogaps pH sensor. All these measurements were made at room temperature. Changes in electrical current determine the operation of the pH sensor.

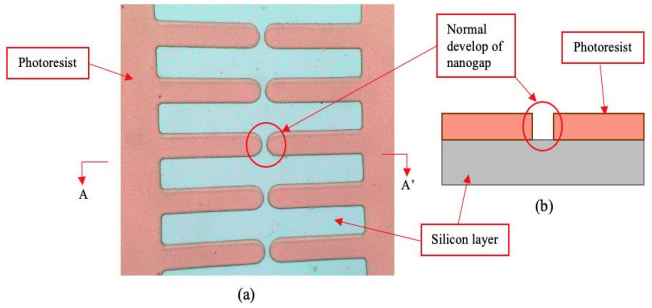

Figure 8. (a) Normal-develop structures of photoresist nanogaps with (b) its cross-section at A-A'

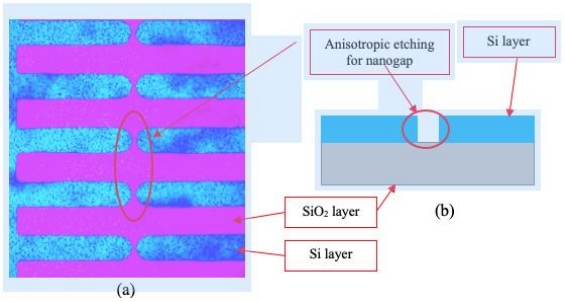

Figure 9. (a) Anisotropic etching result of nanogaps with (b) its cross-section at A-A'

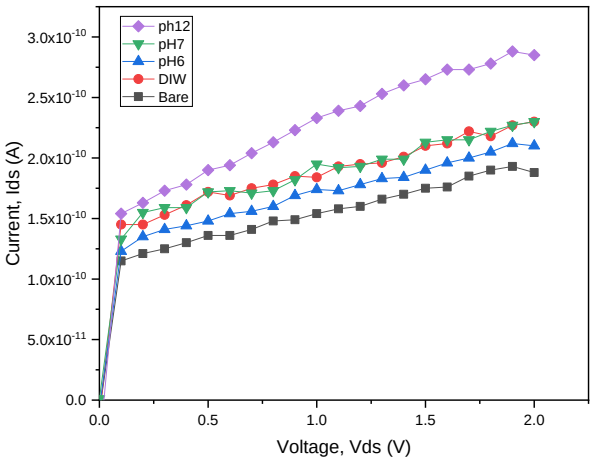

Figure 10. Id_s-V_{ds} (I-V) characteristic of the fabricated silicon nanogaps pH sensor

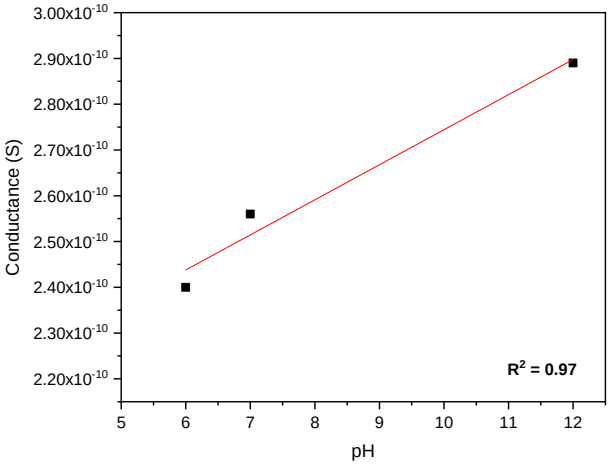

Figure 11. The sensitivity of the silicon nanogaps pH sensor

For each measurement, a 0.5 L droplet of three different pH solutions (pH = 6, 7 and 12) was applied to the silicon nanogaps surface to accomplish the pH electrical characterizations. Based on Figure 10, I-V characteristics indicate an almost linear relationship (ohmic behaviour) [13], [14]. The I_{ds} of pH7 are almost the same as the I_{ds} of DI water showing that DI water is a neutral solution. The measured I_{ds} for pH6, pH7 and pH12 at 2.0 V (V_{ds}) were 210 pA, 230 pA and 285 pA, respectively. The trend for I_{ds} of pH6 is lower than the drain current of pH7 and the trend for pH12 is higher drain current. The result is in agreement with the previous research reported by the researchers [13], [14].

Furthermore, the pH sensitivity of the silicon nanogaps by detecting the changes in the conductance with response to various pH buffer solutions was investigated as shown in Figure 11. The results show that the conductance values changed with different pH buffer solutions (linear relation between the conductance and pH) [15], [16]. The sensitivity of the silicon nanogaps is the slope of the calibration curve. It was observed that I_{ds} increase linearly with increasing pH levels (pH6, pH7, and pH12) with an outstanding sensitivity of 7.66 pS/pH (R^2 = 0.97). To the best of our knowledge, the sensitivity demonstrated in pH detection is among the best, as compared to the previously reported findings [16].

3.3. Simulation of the Silicon Nanogap Biosensors

The silicon nanogap biosensor has been simulated and the effects of the various Qf were demonstrated. Qf was represented as the analyte of the negative biomolecule [17], specifically RBP4. Qf_1, Qf_2, Qf_3, Qf_4, and Qf_5, were 0×10^{10} e/cm^{-2}, -5×10^{11} e/cm^{-2}, -5×10^{12} e/cm^{-2}, -5×10^{13} e/cm^{-2}, -5×10^{14} e/cm^{-2}, respectively. The 3D graphics of the simulated silicon nanogap as shown in Figure 12(a) and (b) show the 3D graphics of the simulated silicon nanogap with Qf on the nanogap surface. Furthermore, Figure 13 shows the I-V characteristic of simulated silicon nanogaps biosensors according to different concentrations of Qf. At V_{ds} = 2 V, the I_{ds} of Qf_1, Qf_2, Qf_3, Qf_4, and Qf_5 were 3.85×10^{-5} A, 4.38×10^{-5} A, 5.24×10^{-5} A, 5.51×10^{-5} A, and 6.21×10^{-5} A respectively. The Qf_5 has been presented with a

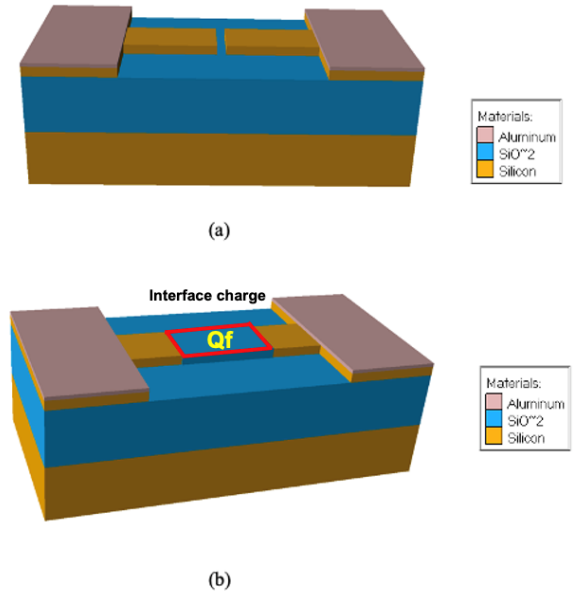

Figure 12. (a) 3D view of the silicon nanogap and (b) interface charge, Qf on the nanogap surface

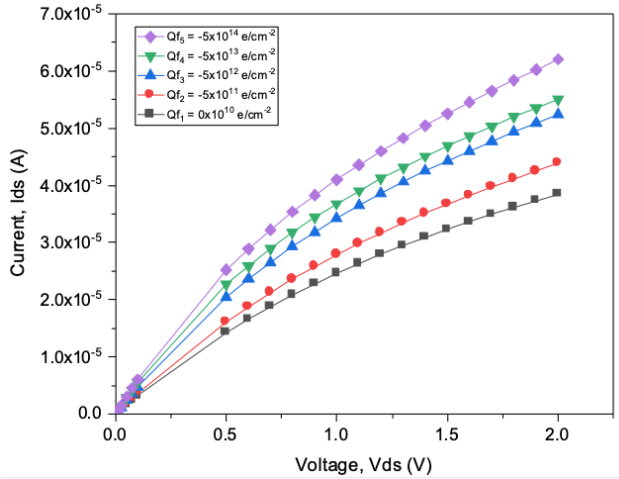

Figure 13. I-V characteristic of silicon nanogaps biosensor according to different concentrations of interface charge density, Qf

more negative interface charge while the Qf_2 has been presented with a less negative interface charge. Qf_1 was defined as a bare device, which implies it has no reaction on the nanogap [18].

Based on the results, the characteristic shows an ohmic behaviour. As expected, the Qf increases with increasing the I_{ds} of the silicon nanogaps. It is because, by adding more negative charge on the surface, more current flows through silicon nanogap from drain to source, resulting in an increasing I_{ds} [19].

In addition, the sensitivity of the silicon nanogap by detecting the changes in I_{ds} in response to various Qf has been analysed as shown in Figure 14. The sensitivity can be determined from the slope of the calibration curve of the silicon nanogaps biosensor. It can be observed the I_{ds} increased linearly with a concentration of negative Qf [20] with an outstanding sensitivity of 3.24 μA/e.cm² (R^2 = 0.98).

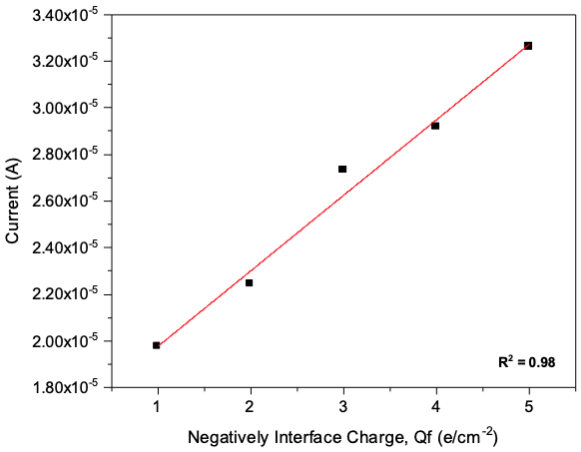

Figure 14. The calibration curve (sensitivity) of the silicon nanogap biosensor

4. CONCLUSION

The fabrication method of a p-type silicon nanogap pH sensor has been reported in this work as a preliminary investigation of RBP4 detection. Top-down conventional lithography and the RIE process were used to fabricate the silicon nanogaps. The silicon nanogap pH sensor was successfully fabricated with a gap range of 100 nm to 200 nm. By measuring the electrical detection in response to various pH levels, this silicon nanogap has been fully demonstrated as a pH sensor. The conductance against pH level was extracted from the I-V graph to calculate the sensitivity. The trend of I-V characteristics for the silicon nanogap pH sensor shows it functions well according to pH level detection. The sensitivity of this silicon nanogap pH sensor was 7.66 pS/pH. In the simulation, the current against concentration was extracted from the I-V graph to calculate the sensitivity of the nanogap at different concentrations (Qf_1, Qf_2, Qf_3, Qf_4, and Qf_5) that represented the negative biomolecule analyte (RBP4). The sensitivity of the silicon nanogap was 3.24 μA/e.cm². In summary, these silicon nanogap pH sensors have shown valuable potential as a biosensor and can potentially be employed as a diagnostic platform for DM.

ACKNOWLEDGMENTS

I would like to acknowledge the Fundamental Research Grant Scheme (FRGS) support under grant number FRGS/1/2020/STG01/UNIMAP/02/1) from the Ministry of Higher Education, Malaysia. The authors also would like to acknowledge all the team members in INEE and, FKTEN, UniMAP for their guidance and help related to this study.

REFERENCES

[1] A. Paul, M. S. Chiriacò, E. Primiceri, D. N. Srivastava, and G. Maruccio, "Picomolar detection of retinol binding protein 4 for early management of type II diabetes," *Biosensors and Bioelectronics*, vol. 128, pp. 122–128, 2019.

[2] M. Nayak, A. Kotian, S. Marathe, and D. Chakravortty, "Detection of microorganisms using biosensors—A smarter way towards detection techniques," *Biosensors and Bioelectronics*, vol. 25, no. 4, pp. 661–667, 2009.

[3] S. Kidambi and S. B. Patel, "Diabetes Mellitus," *The Journal of the American Dental Association*, vol. 139, pp. 8S-18S, 2008.

[4] American Diabetes Association, "Diagnosis and classification of diabetes mellitus.," *Diabetes care*, vol. 33 Suppl 1, no. Suppl 1, pp. S62-9, 2010.

[5] H. M. Naylor and M. E. Newcomer, "The Structure of Human Retinol-Binding Protein (RBP) with Its Carrier Protein Transthyretin Reveals an Interaction with the Carboxy Terminus of RBP," *Biochemistry*, vol. 38, no. 9, pp. 2647–2653, 1999.

[6] S. J. Lee, J.-W. Park, I.-A. Kim, B.-S. Youn, and M. B. Gu, "Sensitive detection of adipokines for early diagnosis of type 2 diabetes using enzyme-linked antibody-aptamer sandwich (ELAAS) assays," *Sensors and Actuators B: Chemical*, vol. 168, pp. 243–248, 2012.

[7] M. Yuqing, C. Jianrong, and F. Keming, "New technology for the detection of pH," *Journal of Biochemical and Biophysical Methods*, vol. 63, no. 1, pp. 1–9, 2005.

[8] T. S. Dhahi, T. Adam, and U. Hashim, "In-House fabrication and Electrical characterization of planner si-nanogap," *Journal of Physics: Conference Series*, vol. 908, p. 012064, 2017.

[9] X. Chen *et al.*, "Electrical nanogap devices for biosensing," *Materials Today*, vol. 13, no. 11, pp. 28–41, 2010.

[10] M. N. F. Zulkiffli *et al.*, "Top-Down Fabrication of Silicon Nanogap for Detection of Dengue Virus (DENV)," in *Embracing Industry 4.0*, Lecture Notes in Electrical Engineering, vol. 678, Springer, Singapore, 2020, pp. 41–49.

[11] R. Torabi and H. Ghourchian, "Ultrasensitive nano-aptasensor for monitoring retinol binding protein 4 as a biomarker for diabetes prognosis at early stages," *Scientific Reports*, vol. 10, no. 1, p. 594, 2020.

[12] Q. Yang *et al.*, "Quantitative Measurement of Full-Length and C-Terminal Proteolyzed RBP4 in Serum of

Normal and Insulin-Resistant Humans using a Novel Mass Spectrometry Immunoassay," *Endocrinology*, vol. 153, no. 3, pp. 1519–1527, 2012.

[13] H. Fujii, S. Kanemaru, H. Hiroshima, S. M. Gorwadkar, T. Matsukawa, and J. Itoh, "Fabrication and characterization of a nanogap edge emitter with a silicon-on-insulator wafer," *Applied Surface Science*, vol. 146, no. 1–4, pp. 203–208, 1999.

[14] Z. Gao *et al.*, "Silicon Nanowire Arrays for Ultrasensitive Label-Free Detection of DNA," in *TRANSDUCERS 2007 - 2007 International Solid-State Sensors, Actuators and Microsystems Conference*, IEEE, 2007, pp. 2003–2006.

[15] M. N. M. Nuzaihan, U. Hashim, A. Ruslinda, M. K. Arshad, and M. H. A. Baharin, "Fabrication of Silicon Nanowires Array Using E-beam Lithography Integrated with Microfluidic Channel for pH Sensing," *Current Nanoscience*, vol. 11, no. 2, pp. 239–244, 2015.

[16] T. Adam and U. Hashim, "Highly sensitive silicon nanowire biosensor with novel liquid gate control for detection of specific single-stranded DNA molecules," *Biosensors and Bioelectronics*, vol. 67, pp. 656–661, 2015.

[17] M. F. M. Fathil *et al.*, "The impact of different channel doping concentrations on the performance of polycrystalline silicon nanowire field-effect transistor biosensor," in *AIP Conference Proceedings*, 2018, p. 020006.

[18] R. F. Abdullah *et al.*, "The impact of silicon nanowire transducer channel width on field-effect transistor biosensor performance," in *AIP Conference Proceedings*, 2021, p. 020251.

[19] C. C. Ong *et al.*, "Field-Effect Transistor-based Biosensor Optimization: Single Versus Array Silicon Nanowires Configuration," in *Embracing Industry 4.0, Lecture Notes in Electrical Engineering*, vol. 678, Springer, Singapore, 2020, pp. 31–40. doi: 10.1007/978-981-15-6025-5_3.

[20] M. E. Ali, T. S. Dhahi, R. Das, and U. Hashim, "DNA hybridization detection using less than 10-nm gap silicon nanogap structure," *Sensors and Actuators A: Physical*, vol. 199, pp. 304–309, 2013.